Ekoloji 27(106): 817-825 (2018)

Low-field NMR Ecological Research on the Effects of Confining Pressure Changes on Pore Fissure Characteristics of High-rank Coal

Ming Yang [1,2,3*], Jingcang Bi [3], YaPeng Liu [3], Xiaomin Jin [3]

[1] The Collaborative Innovation Center of Coal Safety Production of Henan, Jiaozuo Henan 454003, CHINA

[2] State Key Laboratory Cultivation Base for Gas Geology and Gas Control, Henan Polytechnic University, Jiaozuo Henan 454003, CHINA

[3] School of Safety Science and Engineering, Henan Polytechnic University, Jiaozuo Henan 454003, CHINA

[*] Corresponding author: yming2005@163.com

Abstract

Ecologically, the pore fissure system of a coal reservoir is the accumulation place and migration channel of coalbed methane. Pore fissure distribution and environmental characteristics play important roles in enrichment and osmosis migration of coalbed methane. Surrounding stress of coal reservoir is important to internal pore fissure system development in environment. The ecological variation law of pore fissure characteristics of coal samples with and without 1–9 MPa of confining pressure was analyzed through low-field nuclear magnetic resonance experiments to reveal the influence of confining pressure changes on pore fissure characteristics of high-rank coal. Results demonstrated that with the increase of confining pressure, pore volume in coal samples decreases and pore size distribution changes. A few small pores will be converted into large pores, and porosity gradually decreases in the power function form. The proportion of small pores increases, whereas those of middle and large pores decrease. The internal pore connectivity of ecological coal samples is enhanced accompanied with different variation trends of permeability. Corresponding environmental causes were further analyzed.

Keywords: coal reservoir, confining pressure, pore fissure characteristics, permeability, low-field NMR

Yang M, Bi J, Liu Y, Jin X (2018) Low-field NMR Ecological Research on the Effects of Confining Pressure Changes on Pore Fissure Characteristics of High-rank Coal. Ekoloji 27(106): 817-825.

INTRODUCTION

Coal reservoir is a dual-structure ecological system composed of pore and fracture. High-rank coal reservoir is the cleat porosity reservoir, which is characterized by low porosity and permeability, strong heterogeneity, a high degree of metamorphism, large coalbed adsorption quantity, and high substrate density (Zhang 2009). Coalbed methane accumulates and migrates to the pore–fracture environment in a coal reservoir. Pore fissure distribution and structure can directly affect the enrichment and osmosis migration of coalbed methane (Qi 2015). The coal reservoir is strongly sensitive to stress because the pore–fracture system with low intensity will produce large landfill deformations under effective stress (Chen et al. 2008, Liuet al. 2013, Meng and Hou 2012). Confining pressure, temperature stress, and axial stress significantly affect the development and deformation of the pore–fracture system in the coal reservoir environment.

Many ecological studies on the sensitivity of confining pressure in pores and fractures have been reported. Somerton et al. (1975) tested permeability by setting different confining pressures, thus obtaining the empirical formula of confining pressure and permeability. Fatt and Davis (1952) conducted a related ecological experiment based on core and disclosed the variation laws of core porosity and permeability with confining pressure. Osorio et al. (1997) concluded from experimental studies that permeability loss of tight sandstones in gas reservoir is significant with the increase of confining pressure. Peng et al. (2008) found a negative exponent relation between permeability and confining pressure based on permeability changes of coal samples in different ecological sizes during loading and unloading conditions of confining pressure. Lyu et al. (2013) carried out coal core pore permeability tests

 Received: 18 Jun 2016 / Accepted: 10 Oct 2018

under different confining pressures and found that core pore permeability of coal continuously declines with the increase of environment confining pressure. Damages of permeability confining pressure are ecologically more serious than those of porosity confining pressure. However, confining pressure of various coalbed has different sensitivities. Chen et al. (2008) well discussed the influences of coal reservoir's sensitivity to confining pressure on the output of coalbed methane by numerical simulation. They found that coal reservoir has a strong ecological sensitivity to confining pressure and such sensitivity is irreversible. Zhang et al. (2008) conducted an experimental study on the sensitivity of coalbed methane to the confining pressure of dry and wet cores by changing confining and pore pressures. The variation law for permeability with effective pressure can be disclosed based on experimental data fitting. The preceding research findings mentioned well disclosed the relationship between permeability and sensitivity to confining pressure.

According to the literature review, previous ecological studies only focused on the relationship between coal permeability and externally applied load. Pore fissure characteristic parameters of coal reservoir include porosity, permeability, and pore size distribution. In this study, variation laws of pore fissure characteristic parameters, including porosity, permeability, and pore size distribution when external load is applied, were studied through low-field nuclear magnetic resonance (NMR) experiments and imaging techniques. Research results can provide references to study the gas adsorption capacity of high-rank coal, prediction of coal gas outburst risks, coalbed methane evaluation and development, and coal gas discharge (Zhang et al. 2008). Such results have important theoretical significance and practical values.

PRINCIPLE OF LOW-FIELD NMR EXPERIMENTS

NMR is a physical phenomenon in which spectral signal is generated by the interaction between nucleus with odd nucleons (e.g., ^{1}H, ^{13}C, ^{19}F, and ^{31}P) as the spinning nucleus at a very low frequency (VLF) (Zhang 2010). In coal, low-field NMR detects the NMR signal of 1H in the coal pores of saturated water using the low-intensity magnetic field to acquire the spectrum of transverse relaxation time (T_2), that is, the T_2 spectrum of water in saturated water coal. This T_2 spectrum is used to analyse pore size distribution, connectivity, and physical characteristics of coal samples (He et al. 2005).

Relaxation time refers to the time for the magnetization vector to recover from an excited to an equilibrium state. Moreover, relaxation time includes transverse relaxation time (T_2) and longitudinal relaxation time (T_1). NMR is mainly used to test T_2 in coal (Sun et al. 2015). The three types of T_2 relaxation mechanisms are free, surface, and diffusion relaxations (Coates et al. 1993), which can be expressed as follows:

$$\frac{1}{T_2} = \frac{1}{T_{2F}} + \frac{1}{T_{2S}} + \frac{1}{T_{2D}} \quad (1)$$

where T_2 is the transverse relaxation time of the porous fluid collected by CPMG sequence, T_{2F} is the free relaxation time, T_{2S} is the surface relaxation time, and T_{2D} is the diffusion relaxation time.

T_{2F} and T_{2D} are determined by the physical properties (e.g., chemical components and viscosity) of fluid, and experiments are generally performed in the uniform magnetic field; thus, influences of free and diffusion relaxations can be neglected. T_{2S} is the relaxation effect of coal pore surface on fluids and is related with the specific surface area of pores. Also takes the dominant role in relaxation. Consequently, Eq. (1) can be simplified into:

$$\frac{1}{T_2} \approx \frac{1}{T_{2S}} = \rho_2 \times \left(\frac{S}{V}\right) \times P \quad (2)$$

where ρ_2 is the surface relaxation rate of coal samples, and $(S/V) \times P$ is the specific surface area of pores. Suppose pore is a cylinder with a radius of R. Then, Eq. (2) can be further simplified as follows:

$$T_2 = F_S \times R \quad (3)$$

$$F_S = \frac{1}{2\rho_2} \quad (4)$$

In Eq. (3) and (4), T_2 distribution is related to pore size. A large aperture is accompanied with a high T_2 and a long water relaxation time in the pore, while a small aperture leads to a small T_2, a strong confining pressure to water in the pore, and a short relaxation time. Hence, relaxation peak position is related with aperture. The peak area is related with aperture (Shi and Pan 2005, Xiao 1996). According to the literature review (Xie et al. 2015), the surface relaxation rate of high-rank coal core is ρ_2 =5.4μm/s. Therefore, the T_2 spectrum can be converted into the pore size distribution map of a coal sample.

Core porosity is measured by the low-field NMR technique. Generally, core samples are vacuumed and then saturated. Therefore, the pore volume is equal to the saturated water volume of samples. Saturated water

volume can be tested by the NMR. A high porosity represents a high saturated water volume, and the measured NMR signal is strong. The relation curve (standard sample curve) between the NMR signal strength and porosity can be obtained by testing (generally 3–6) NMR signals of samples with a certain volume and known porosity. Then, samples with unknown porosity could be measured by the standard sample curve, thus calculating the porosity of samples (Xiao 2012, Zhu et al. 2013).

Coates model is used to calculate NMR permeability (Huang et al. 2004). Pore size parameters are implicitly inputted through the T_2 cut-off value, which determines FFI/BVI.

In Coates model, permeability (K) is expressed as follows:

$$K = \left(\frac{\phi}{C}\right)^4 \times \left(\frac{FFI}{BVI}\right)^2 \quad (5)$$

where ϕ is the porosity, C is the coefficient and empirical parameter that varies for different samples, FFI is free fluid saturation, and BVI is bound fluid saturation.

EXPERIMENTAL CONTENT

Experimental Preparation

In this experiment, MesoMR23-060H-I low-field NMR spectrometer manufactured by Shanghai Niumag Corporation was applied. The resonant frequency was 21.67568 MHz. The magnetic temperature was controlled at 31.99–32.01 °C. The magnetic field intensity was 0.5 T. The RF pulse frequency was 21.67568 MHz. The T2 spectrum of the sample was tested by the low-field NMR spectrometer. CPMG sequence parameters of samples were tested: SW = 333.333 KHz, TE = 0.406 ms, NS = 32, TW = 3000 ms, NECH 10000, RG1 = 15 db, DRG1=3, DR = 1, PRG = 0 and $T_{2cutoff}$ = 4 ms (Xiao and Xiao 2008). Sample saturation was accomplished by a vacuum saturation device, and samples were dried in a vacuum drying oven.

Experimental Steps

First, coal samples were collected from Zhaogu Mine 1 (ZG1), Zhaogu Mine 2 (ZG2), Shanxi Wangtaipu Mine (WTP), and Jiulishan Mine (JLS) and then prepared into Φ25 mm × 50 mm standard sizes. These samples were respectively marked as ZG1-W, ZG2-W, WTP-W, and JLS-W. Second, coal samples were dried in an electrothermal blowing dry box for 12 h, saturated for 12 h in a vacuum saturation device, and soaked in water for 24 h until the coal mass remained the same and reached the saturation state. Third, the instrument was started and calibrated. A porosity standard line was created. Finally, the saturated coal samples were wrapped by a plastic film and then placed in the experimental platform. T_2 spectra, porosity, permeability, and pore size distribution of coal samples were tested under different confining pressures (0, 1, 3, 5, 7, and 9 MP).

TEST RESULTS AND ANALYSIS

T_2 Spectrum under Different Confining Pressures

Test results

T_2 spectra of coal samples from four mines under different confining pressures were tested. T_2 spectra distributions and calculated area under different confining pressures are shown in **Fig. 1** and **Table 1**, respectively.

Analysis of test results

Table 1 and **Fig. 1** show the T_2 spectra changes of coal samples from four mines under the application of confining pressure. With the increase of confining pressure, the first peak of T_2 spectra gradually decreases and peak area successively shrinks. In addition, all spectrum shapes have a certain rightward offset. T_2 spectra of JLS-W and ZG2-W have new peaks at the most right sides. According to the NMR principle, peak area represents pore volume in coal samples, which reveals a negative correlation between confining pressure and pore volume in coal samples. Pore size distribution changes and a few small pores will be converted into large one.

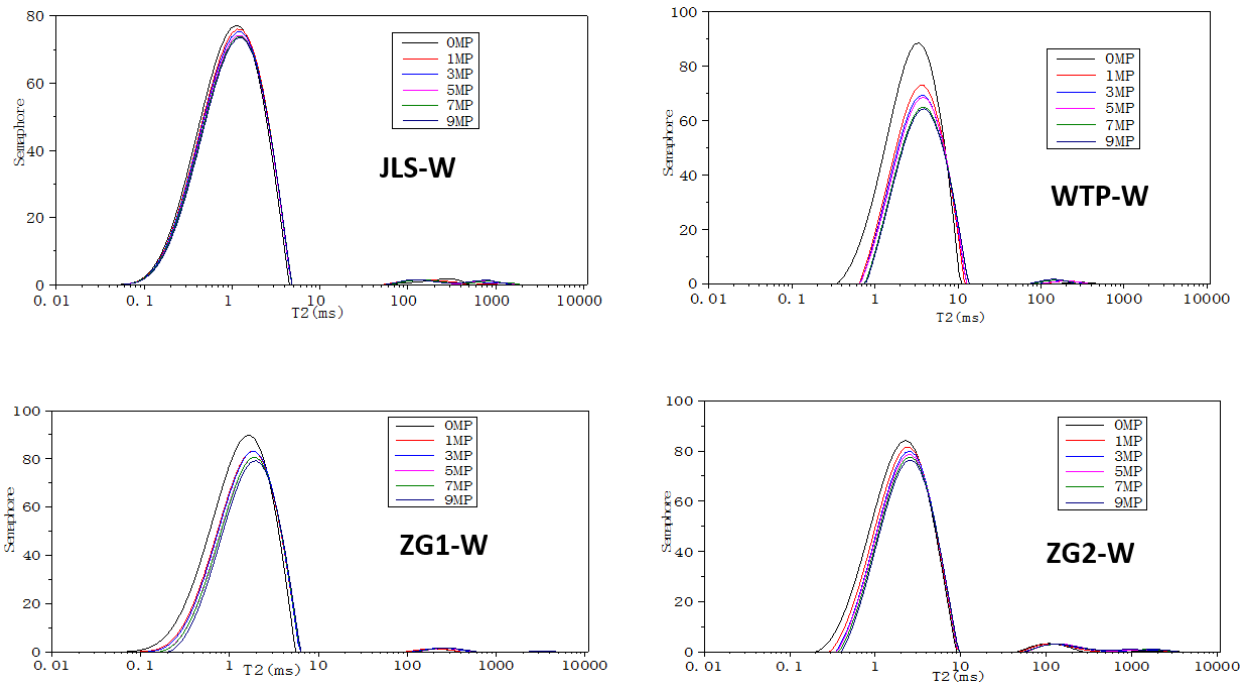

Fig. 1. T_2 spectra of coal samples under different confining pressures

Table 1. T_2 area of coal samples under different confining pressures

Area T_2 / Number / Pressure (Mpa)	JLS-W	WTP-W	ZG1-W	ZG2-W
0	2363.468	2320.092	2549.288	2439.487
1	2353.843	1819.758	2298.527	2282.017
3	2319.496	1745.118	2273.639	2187.172
5	2283.458	1719.503	2175.101	2158.797
7	2280.503	1616.401	2169.449	2108.759
9	2257.443	1590.174	2092.431	2061.505

Table 2. Test results of porosity under different confining pressures

Number / Pressure (Mpa)	JLS-W		ZG1-W		ZG2-W		WTP-W	
	Porosity /%	Decreasing amplitude/%	Porosity /%	Decreasing amplitude/%	Porosity /%	Decreasing amplitude/%	Porosity /%	Decreasing amplitude/%
0	5.525	0	6.564	0	6.962	0	6.118	0
1	5.499	0.47	5.952	9.32	6.441	7.48	5.215	14.76
3	5.488	0.2	5.891	1.02	6.111	5.12	5.02	3.74
5	5.402	1.57	5.611	4.75	5.983	2.09	4.894	2.51
7	5.386	0.3	5.58	0.55	5.792	3.19	4.423	9.62
9	5.345	0.76	5.374	3.69	5.599	3.33	4.326	2.19
Total decrease		3.26		18.13		19.58		29.29

Effects of Confining Pressure on Porosity

Test results

Table 2 shows the test results of porosity under different confining pressures. Therefore, the relation curve between porosity and confining pressure can be obtained (**Fig. 2**).

Analysis of test results

Fig. 2 shows that porosity of all four samples changes in the same trend with the increase of confining pressure. Hence, porosity declines in the power function form with the increase of confining pressure. Moreover, porosity rapidly declines when the confining pressure is smaller than 4 MPa but slowly declines and stabilizes when the confining pressure is higher than 4 MPa.

NMRI Results of Coals under Different Confining Pressures and Analysis

NMRI results

In this paper, pore fissure characteristics on axial profiles of ZG1-W, ZG2-W, WTP-W, and JLS-W with

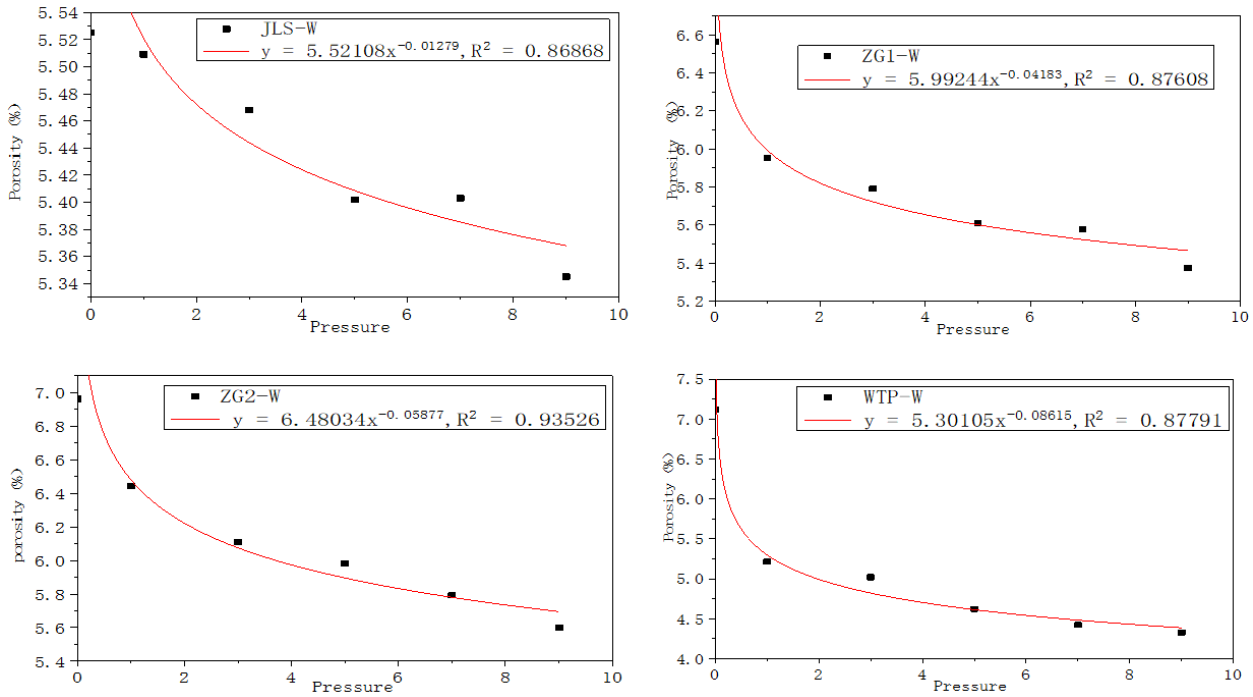

Fig. 2. Map of the relationship between porosity and pressure

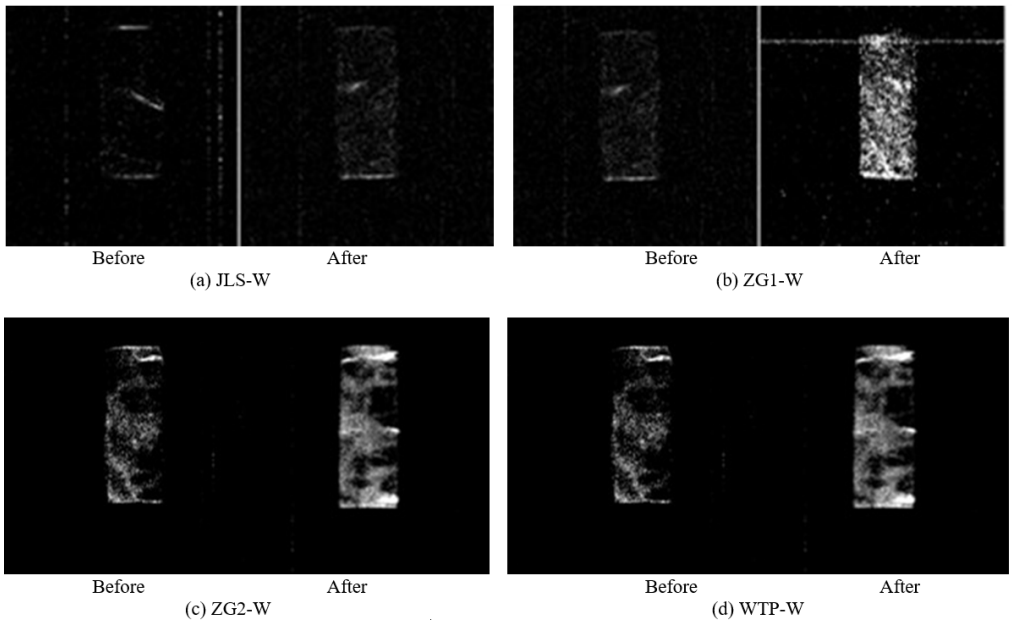

Fig. 3. NMR imaging of coal samples before and after pressure

or without the application of 9 MPa confining pressure were analysed by the NMRI technique. **Fig. 3** shows the pore fracture structural images before and after the application of confining pressure. Bright spots are pores and fractures of samples.

Analysis of NMRI results

In **Fig. 3**, the images of four coal samples before and after the application of confining pressure have obvious differences. The images contain more bright spots after the application of confining pressure than prior, thereby indicating that internal pore connectivity is enhanced with the increase of confining pressure. According to the related literature (Liu 2011), this paper focused on the influence of confining pressure on pore size distribution in the range over 10 nm because the experimental pressure slightly influences micropore. The variation trends of small pores (10-100 nm) and middle and large pores (> 100 nm) can be acquired according to low-field NMR experimental results, as shown in **Fig. 4** and **Fig. 5**.

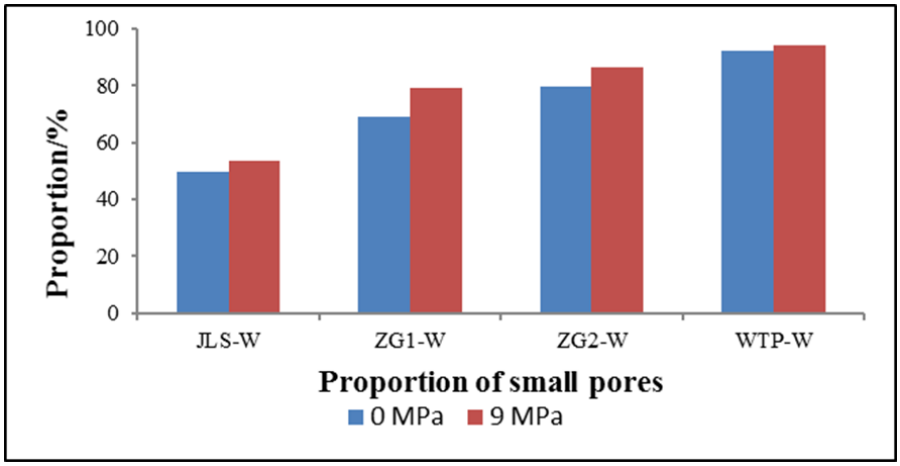

Fig. 4. Variation trend of the hole (10–100 nm) of different coal sample proportions with increasing confining pressure

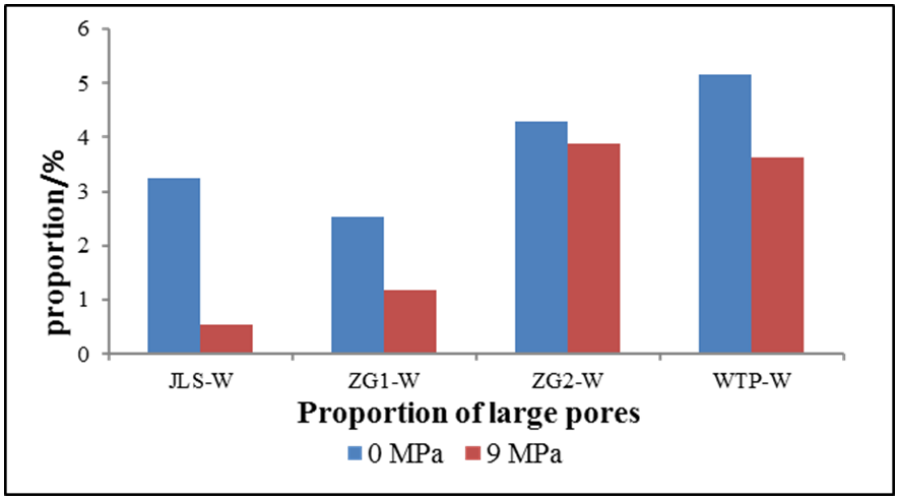

Fig. 5. Variation trend of the hole (> 100 nm) of different coal sample proportions with increasing confining pressure

Table 3. Test results of permeability under different confining pressures

Permeability / Number / Pressure (Mpa)	JLS-W	WTP-W	ZG1-W	ZG2-W
0	0.212	2.705	121.871	506.296
1	0.383	6.009	114.864	293.479
3	0.396	6.244	109.9	283.026
5	0.454	6.622	107.545	307.921
7	0.51	6.419	104.194	223.227
9	0.553	6.605	97.744	213.887

In **Fig. 4** and **Fig. 5** the proportion of small pores is positively related with confining pressure, while those of middle and large pores are negatively related.

According to NMRI analysis and pore size distribution, the proportion of small pores increases with the increase of confining pressure, whereas those of the middle and large pores decrease. The internal porosity connectivity of coal samples is enhanced.

Effects of Confining Pressure on Permeability

Test results

The porosity of four coal mines under different confining pressures is tested. **Table 3** lists the results.

Result analysis

The relationship between permeability and confining pressure can be acquired (**Fig. 6**) based on permeability test results under different confining pressures (**Table 3**).

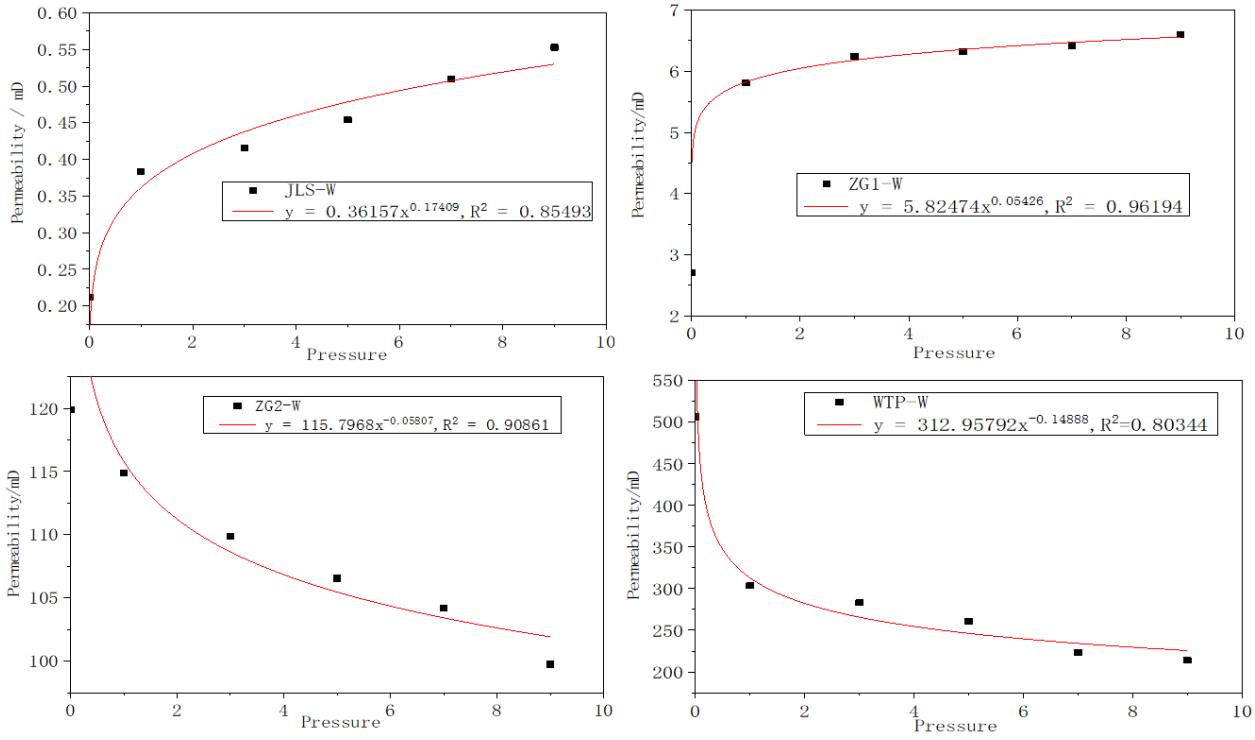

Fig. 6. Map of the relationship between permeability and pressure

Table 4. Calculation results of FFI/BVI value of coal samples under different confining pressures

Number / Pressure (Mpa)	JLS-W		ZG1-W		ZG2-W		WTP-W	
	FFI/BVI	**Amplitude /%**	***FFI/BVI***	**Amplitude /%**	***FFI/BVI***	**Amplitude /%**	***FFI/BVI***	**Amplitude /%**
0	0.0151	0	0.0382	0	0.2143	0	0.4441	0
1	0.02	32.45	0.0692	81.15	0.2583	20.53	0.6299	41.84
3	0.0209	4.5	0.072	4.05	0.2807	8.67	0.6676	5.99
5	0.0231	10.53	0.0817	13.47	0.2897	3.21	0.6941	3.97
7	0.0245	6.06	0.0821	0.49	0.3043	5.04	0.7637	10.03
9	0.0261	6.53	0.089	8.4	0.3154	3.65	0.7815	2.33
Total Amplitude		72.85		132.98		47.18		75.97

In **Fig. 6**, the permeability of four coal samples show two different variation trends under different confining pressures. With the increase of confining pressure, the permeability of JLS-W and ZG1-W gradually increases, whereas that of ZG2-W and WTP-W gradually decreases.

Cause of different variation trends of permeability

From Eq. (5), the NMR calculation model of permeability is as follows:

$$K = \left(\frac{\phi}{C}\right)^4 \times \left(\frac{FFI}{BVI}\right)^2 \quad (6)$$

FFI/BVI values under different confining pressures can be calculated according to the numerical values of *FFI* and *BVI* measured by low-field NMR experiments (**Table 4**).

In **Table 4**, FFI/BVI is positively correlated with confining pressure, thereby indicating that free fluid space in coals relatively increases. *FFI/BVI* values of JLS-W, ZG1-W, ZG2-W, and WTP-W under 9 Mpa increase by 72.85%, 132.98%, 47.18%, and 75.97%, respectively, compared with those under 0 Mpa.

According to **Table 2**, the porosity of JLS-W, ZG1-W, ZG2-W, and WTP-W decreases by 3.26%, 18.13%, 19.58%, and 29.29%, respectively, with the increase of confining pressure.

In Eq. (6), K is proportional to the fourth power of ϕ and is positively correlated with the square of FFI/BVI. Hence, test results of permeability are influenced by ϕ and FFI/BVI. Variations of FFI/BVI and ϕ demonstrate that FFI/BVI of JLS-W and ZG1-W decreases more than ϕ, thereby resulting in the growth of permeability with the increase of confining pressure. However, the reduction of ϕ takes the dominant role for WTP-W and ZG2-W, which results

in the decrease of permeability with the increase of confining pressure.

Permeability is sensitive to porosity, effective porosity, and *BVI* according to permeability test results of low-field NMR experiments. Different influencing factors have different influencing mechanisms, thus resulting in different variation trends of permeability.

CONCLUSIONS

(1) In NMR ecological experiments, confining pressure can significantly influence pore structure. With the increase of confining pressure, the pore volume of coal samples decreases in environemnt. Porosity decreased in the power function form accordingly. Porosity rapidly declines when the confining pressure is smaller than 4 MP but slowly decreases and stabilizes when the confining pressure is higher than 4 MP.

(2) Bright spots in NMR ecological images increase with the increase of confining pressure, thereby indicating that internal pore connectivity is enhanced. According to environmental changes in pore size distribution, the proportion of small pores in all four samples increases, while those of the middle and large pores decrease.

(3) Permeability variations of different coal samples differ with the increase of confining pressure. Permeability increases for a coal sample with small permeability and decreases for coal samples with large permeability. Causes of such ecological variation trends are further analyzed. Therefore, such variation trends are attributed to the permeability calculation formula of the NMR model.

ACKNOWLEDGEMENTS

This work was sponsored by the National Nature Science Foundation of China (51734007, 51704099, and 51604096), Program for Innovative Research Team in University of Ministry of Education of China (IRT_16R22), Henan Province University Science and Technology Innovation Team (17IRTSTHN030) , the Basic and Frontier Technology Research Project of Henan Province (142300413233), and the Doctoral Fund of Henan Polytechnic University (B2015-09). We are very grateful to them for their support.

REFERENCES

Chen ZH, Wang YB, Guo K, Sun QP, Zhang YP (2008) Acta Geologica Sinica, 82(10): 1390.
Coates GR, Xiao LZ, Prammer MG (1993) NMR Logging Principles and Applications. Houston.
Fatt I, Davis DH (1952) Journal of Petroleum Technology, (14): 16.
He YD, Mao ZQ, Xiao LZ, Ran XJ (2005) Chinese Journal of Geophysics, 48(2): 373.
Huang QS, Zhao WJ, Yang JQ, Liu BK (2004) Journal of Qingdao University (Natural Science Edition), 17(4): 37.
Liu AH, Fu XH, Liang WQ, Lu L, Luo PP (2013) Coal Science and Technology, 41(4): 104.
Liu YW (2011) Henan Polytechnic University, China.
Lv YM, Tang DZ, Xu H (2013) Coal Geology & Exploration, 41(6): 31.
Meng ZP, Hou QL (2012) Journal of China Coal Society, 37(3): 430.
Osorio JG, Chen HY, Teufel LW (1997) Numerical Simulation of Coupled Fluid-Flow/Geomechanical Behavior of Tight Gas Reservoirs with Stress Sensitive Permeability. Presented at the Latin American and Caribbean Petroleum Engineering Conference and Exhibition, Rio de Janeiro, 30 August–3 September. Society of Petroleum Engineers. doi: 10.2118/39055-MS
Peng YW, Qi QX, Deng ZG, Li HY (2008) Journal of China Coal Society, 33(5): 09.
Qi Y (2015) Science and Technology & Innovation, (09): 120.
Shi Q, Pan YS (2005) Coal Mining Technology, 10(6): 10.
Somerton WH, Söylemezoğlu IM, Dudley RC (1975) International Journal of Rock Mechanics & Mining Sciences & Geomechanics Abstracts, (5-6): 29.
Sun XX, Yao YB, Chen JY, Xie SB, Li CC (2015) Geoscience, 29(1): 190.
Xiao F (2012) Yangtze University, China.
Xiao L, Xiao ZX (2008) Progressin Geophysics, 23(1): 167.
Xiao LZ (1996) Well Logging Technology, 20(1): 27.
Xie SB, Yao YB, Chen JY, Yao W (2015) Journal of China Coal Society, 40(S1): 170.
Zhang Y (2009) Chongqing University. China.
Zhang Y (2010) Science & Technology Information, (15): 116.

Zhang YP, He YF, Yang ZM, Liu X (2008) Nat Ural Gas Geoscience, 21(3): 518.
Zhu HL, Zhou KP, Zhang YM, Tian K, Li JL (2013) Chinese Journal of Rock Mechanics and Engineering, 32(7): 1410.